Homogeneous catalytic O_2 reduction to water by a cytochrome *c* oxidase model with trapping of intermediates and mechanistic insights

Zakaria Halime[a,b], Hiroaki Kotani[a], Yuqi Li[b], Shunichi Fukuzumi[a,c,1], and Kenneth D. Karlin[b,c,1]

[a]Department of Material and Life Science, Division of Advanced Science and Biotechnology, Graduate School of Engineering, Osaka University, Advanced Low Carbon Technology Research and Development Program (ALCA), Japan Science and Technology Agency (JST), Suita, Osaka 565-0871, Japan; [b]Department of Chemistry, The Johns Hopkins University, Baltimore, MD 21218; and [c]Department of Bioinspired Science, Ewha Womans University, Seoul 120-750, Korea

Edited by Edward I. Solomon, Stanford University, Stanford, CA, and approved July 6, 2011 (received for review March 24, 2011)

An efficient and selective four-electron plus four-proton ($4e^-/4H^+$) reduction of O_2 to water by decamethylferrocene and trifluoroacetic acid can be catalyzed by a synthetic analog of the heme a_3/Cu_B site in cytochrome *c* oxidase (^{6}LFeCu) or its Cu-free version (^{6}LFe) in acetone. A detailed mechanistic-kinetic study on the homogeneous catalytic system reveals spectroscopically detectable intermediates and that the rate-determining step changes from the O_2-binding process at 25 °C room temperature (RT) to the O-O bond cleavage of a newly observed Fe^{III}-OOH species at lower temperature (−60 °C). At RT, the rate of O_2-binding to ^{6}LFeCu is significantly faster than that for ^{6}LFe, whereas the rates of the O-O bond cleavage of the Fe^{III}-OOH species observed (−60 °C) with either the ^{6}LFeCu or ^{6}LFe catalyst are nearly the same. Thus, the role of the Cu ion is to assist the heme and lead to faster O_2-binding at RT. However, the proximate Cu ion has no effect on the O-O bond cleavage of the Fe^{III}-OOH species at low temperature.

heme/copper | dioxygen reduction | ferric hydroperoxo | kinetic mechanism | enzyme model

The heme/copper (heme a_3/Cu_B) heterodinuclear center in cytochrome *c* oxidases (*Cc*O) (Fig. 1*A*) has attracted much interest, because this is the site where the four-electron and four-proton reduction of dioxygen to water takes place as the final stage of the respiration chain (Eq. **1**).

$$O_2 + 4e^-(\text{from cyt-}c_{\text{reduced}}) + 8\,H^+(\text{from inside membrane}) \rightarrow 2\,H_2O + 4\,H^+(\text{membrane translocated}) + 4\,\text{cyt-}c_{\text{oxidized}}. \quad [1]$$

This exergonic process, occurring without leakage of harmful partially reduced oxygen species, is coupled to the translocation of four additional protons across the membrane, generating a pH gradient and membrane potential which is harnessed through the subsequent synthesis of ATP (1–4).

In addition to protein crystallography, mechanistic enzymology, site-directed mutagenesis, and theoretical calculations, biomimetic inorganic modeling of the *Cc*O active site has been employed. The goal is to provide insights and elucidate mechanisms of the four-electron reduction of O_2 by coordination complexes including heme-Cu assemblies, as may be relevant to biological systems including *Cc*O but also of technological significance such as in fuel cell chemistry (5–7).

A number of heme a_3/Cu_B synthetic analogues have been developed to mimic the coordination environment of the heme a_3/Cu_B bimetallic center in *Cc*O (8–11). The functionality of these analogues has been investigated under two main complementary approaches. One focuses on the generation and characterization of stable O_2-adducts and derived species in heme-copper synthetic assemblies (8, 9). This stoichiometric approach represents an efficient tool to probe the properties and plausibility of the intermediates relevant to the enzyme catalytic cycle and/or O-O reductive cleavage chemistry, the latter of critical importance in chemical and biochemical utilization of molecular oxygen. The second approach, based on electrochemical functional modeling, examines the capability of synthetic models to perform the catalytic four-electron reduction of O_2 (10, 11). However, the solid supported state employed for such studies has precluded any spectroscopic monitoring or intermediates detection. This problem is a major obstacle for the development of kinetics and mechanistic studies in synthetic models or to answer important mechanistic questions such as the role of the Cu_B in the four-electron reduction of O_2.

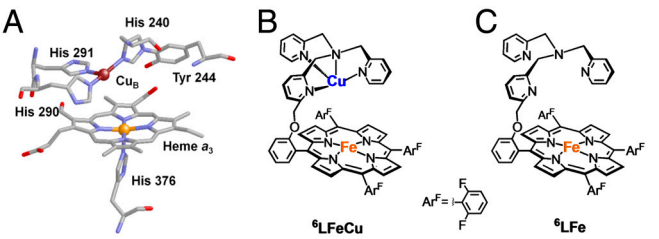

Fig. 1. (*A*) X-ray structures of the fully reduced bimetallic heme a_3/Cu_B center in *Cc*O from bovine heart ($Fe^{II}\cdots Cu^{I} = 5.19$ Å) (3) [figure adapted from (8)]. (*B*) heme/Cu synthetic model for *Cc*O (^{6}LFeCu). (*C*) Cu-free version of synthetic model for *Cc*O (^{6}LFe).

As an alternative to the limitations of the two approaches described above, we report herein an efficient $4e^-/4H^+$ catalytic reduction of O_2 to water, catalyzed by a heme/Cu functional model of *Cc*O (^{6}LFeCu, Fig. 1*B*) and its Cu-free version (^{6}LFe, Fig. 1*C*). As described below, this homogeneous catalytic system has allowed us to develop a detailed kinetic description supported by spectroscopic detection of reactive intermediates overall providing unique mechanistic insights into the O-O reductive cleavage process (12).

We previously reported that the reduced form of $[^6LFe^{II}Cu^{I}]^+B(C_6F_5)_4^-$ reacts with O_2 to form a low-temperature stable $^6LFe^{III}$-μ-peroxo-Cu^{II} ($[^6LFe^{III}$-(O_2^{2-})-$Cu^{II}]^+B(C_6F_5)_4^-$) complex ($\nu_{O\text{-}O} = 808$ cm^{-1}, $\Delta^{16/18}O_2 = -23$ cm^{-1}), deduced to be very similar to a crystallographically characterized Fe^{III}-(μ-η^2:η^1-peroxo)-Cu^{II} complex reported by Naruta and coworkers (13). The $[^6LFe^{III}$-(O_2^{2-})-$Cu^{II}]^+$ complex thermally

Author contributions: S.F. and K.D.K. designed research; Z.H., H.K., and Y.L. performed research; Z.H., H.K., S.F., and K.D.K. analyzed data; and Z.H., S.F., and K.D.K. wrote the paper.

The authors declare no conflict of interest.

This article is a PNAS Direct Submission.

[1]To whom correspondence may be addressed. E-mail: fukuzumi@chem.eng.osaka-u.ac.jp or karlin@jhu.edu.

This article contains supporting information online at www.pnas.org/lookup/suppl/doi:10.1073/pnas.1104698108/-/DCSupplemental.

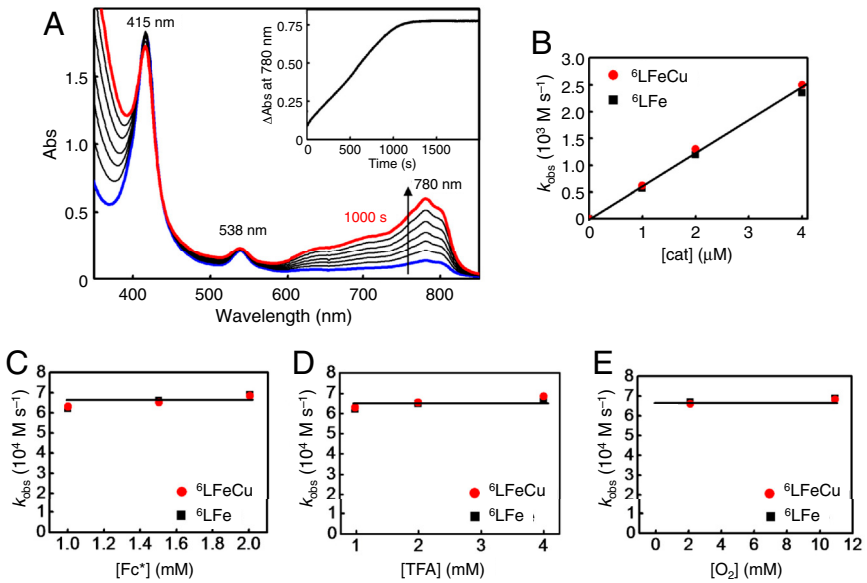

Fig. 2. (*A*) UV-vis spectral changes during the four-electron reduction of O_2 by Fc* (1.0 mM) catalyzed by ^{6}LFeCu (1.0 μM) in the presence of TFA (1.0 mM) in air-saturated acetone ([O_2] = 2.2 mM) at −60 °C. The insert shows the time profile of the absorbance at 780 nm relative to Fc^{*+} formation. Note: a tiny amount of Fc^{*+} is formed (see the nonzero absorbance) during the mixing time following combining catalyst and ferrocene solutions (in order to obtain a homogeneous solution) and before the first spectrum is recorded. Thus, for practical reasons, this first spectrum corresponds to time = 0. (*B*) Plots of k_{obs} vs. [cat] for ^{6}LFeCu and ^{6}LFe^{II} at −60 °C. (*C*) Plots of k_{obs} vs. [Fc*] for ^{6}LFeCu and ^{6}LFe at −60 °C. (*D*) Plots of k_{obs} vs. [TFA] for ^{6}LFeCu and ^{6}LFe^{II} at −60 °C. (*E*) Plots of k_{obs} vs. [O_2] for ^{6}LFeCu and ^{6}LFe at −60 °C.

decomposes releasing $\frac{1}{2}$ equivalent (equiv) of O_2 to generate an Fe^{III}-μ-oxo-Cu^{II} complex ($[^6LFe^{III}\text{-O-}Cu^{II}]^+B(C_6F_5)_4^-$) (14–16). We find that the latter, as a convenient reagent, efficiently catalyzes the $4e^-/4H^+$ reduction of O_2 to water by decamethylferrocene (Fc*) as one-electron donor and trifluoroacetic acid (TFA) as a proton source (Eq. 2).

$$O_2 + 4H^+ + 4Fc^* \xrightarrow{\text{Cat: } ^6\text{LFeCu}} 2H_2O + 4Fc^{*+} \qquad [2]$$

Results and Discussion

Catalytic O_2-Reduction at −60 °C. When the time course for catalytic reaction Eq. 2 is followed by UV-visible spectroscopy at −60 °C (Fig. 2*A*), two main changes occur. There is a rise in the absorbance at 780 nm due to the formation of ferrocenium cation (Fc^{*+}) as product formed following electron-donation by Fc*. The strong absorbance at 415 nm corresponds to the Soret band of the heme in its steady-state form in the catalytic cycle. This reaction intermediate has been determined to be a unique $^6LFe^{III}$-hydroperoxo Cu ($^6LFe^{III}$-OOH Cu) species (415, 538 nm); $\{^6LFe^{III}\text{-OOH }Cu^{II}\}^{2+}$ could be independently generated at low temperature (−80 °C) by the addition of an excess of TFA to the previously described peroxo complex $[^6LFe^{III}\text{-}(O_2^{2-})\text{-}Cu^{II}]^+$ (418, 540, 558 nm) (Fig. S1). The hydroperoxo formulation is further supported by electrospray ionization mass spectrometry (ESI-MS) data and EPR spectroscopic monitoring of its formation (Figs. S2 and S3); the addition of an excess TFA to the EPR-silent $[^6LFe^{III}\text{-}(O_2^{2-})\text{-}Cu^{II}]^+$ complex resulted in the display of a characteristic signal ($g = 6.08$) of a five coordinate high-spin heme and typical signal for the Cu^{II} moiety ($A_{||} = 142 \times 10^{-4}$ cm^{-1}, $A_{\perp} = 12 \times 10^{-4}$ cm^{-1}, $g_{||} = 2.26$ and $g_{\perp} = 2.05$)*. Hydroperoxo complex O-O reductive cleavage by $2Fc^*/3H^+$ (to two waters) leads to $\{^6LFe^{III}Cu^{II}\}^{3+}$ which undergoes further two-electron (2 Fc*) reduction to the fully reduced form $\{^6LFe^{II}Cu^{I}\}^+$; these observations also strongly support the ($^6LFe^{III}$-OOH Cu) steady-state species formulation (Figs. S4, S5).

The stoichiometry of the overall reaction was confirmed by the observation that exactly four equiv of Fc^{*+} form per mole of O_2 reacted (i.e., under limiting [O_2]). H_2O_2 as a product formed via the partial two-electron reduction of O_2 was ruled out by iodometric titration experiments (Fig. S6); no hydrogen peroxide was detected. In addition, it was confirmed that O_2 reduction by Fc* without catalysts (^{6}LFeCu or ^{6}LFe) is negligible under the same conditions (Fig. S6).

To help to examine the role of the Cu in this system, a Cu-free version (^{6}LFe) (15) was also subjected to the same catalytic reaction conditions as ^{6}LFeCu. Even in the absence of Cu the reaction proceeds through the $4e^-$ process (Fig. S7). This result is in accordance with earlier electrochemical studies in which it was found that only the iron porphyrinate itself is essential for O_2 four-electron reduction (17–20). In the case of $^6LFe^{II}$ as well, the kinetics reveal that the Fe^{III}-OOH complex represents the catalytic cycle steady-state species (Fig. S7*A*).

Further kinetic insights demonstrate the reactions being studied are zero-order with respect to Fc^{*+} formation for both ^{6}LFeCu (Fig. 2*A*, inset) and ^{6}LFe (Fig. S7*B*) as catalysts. The derived rate constants increase linearly with an increase in catalyst concentrations (Fig. 2*B*) and also remain constant with a change in the concentration of Fc* (Fig. 2*C*). Further, and to our surprise, the observed zero-order rate constants (k_{obs}) with ^{6}LFeCu at −60 °C are exactly the same as those with the Cu-free complex ^{6}LFe (Fig. 2*B*). Also, the rate of the reaction remains constant with an increase in [TFA] or [O_2] (Fig. 2 *D* and *E*).

These data demonstrate that the rate of O_2-reduction is not affected by the concentrations of O_2, TFA, or Fc*. Thus, the rate-determining step of the catalytic reaction at low temperature is O-O bond cleavage in the steady-state Fe^{III}-OOH species and this is followed by rapid electron transfer to complete the $4e^-$ reduction of O_2. The same k_{obs} value observed for ^{6}LFeCu and

*In $^6LFe^{III}\text{-}(O_2^{2-})\text{-}Cu^{II}$ the high-spin Fe^{III} (d^5, $S = 5/2$) system is strongly antiferromagnetically coupled to the Cu^{II} ion (d^9, $S = 1/2$) through the peroxo bridge, giving an overall $S = 2$ spin system and an EPR-silent spectrum. The addition of the excess of TFA causes the formation of the [Fe^{III}-OOH Cu^{II}] in which the Fe and the Cu are no longer antiferromagnetically coupled and both the high-spin Fe^{III} and the Cu^{II} ion centers independently display an EPR signal (Fig. S3).

^{6}LFe suggests that the Cu is not bound to the Fe^{III}-OOH moiety in {^{6}LFe^{III}-OOH Cu}.

Catalytic O_2-Reduction at 25 °C. The spectral changes observed for the catalytic reaction (Eq. 2) at RT are quite different from those observed at −60 °C. At RT, the Soret band corresponding to the steady-state is observed at 422 nm (Fig. 3*A*), and this can be assigned to the reduced heme (Fe^{II}) (16). Further confirmation comes from spectral correlation with the species generated in the absence of O_2 using Fc* in the presence of TFA (Figs. S5 and S8).

In the presence of excess O_2, the reaction kinetics are zero-order in Fc^{*+} formation (Fig. 3*A*, inset), while the zero-order rate constant increases linearly with an increase in the catalyst concentration (Fig. 3*B*, Fig. S9), as expected. More interestingly, the rate constant also increases with an increase in the O_2 concentration (Figs. 3*E*, Fig. S10), but remains constant with increases in the acid or Fc* concentrations (Fig. 3*C*). On the basis of these observations, and knowing that the reduced heme (^{6}LFe) is the steady-state species observed for the catalytic cycle (*vide supra*), we can conclude that the rate-determining step at 25 °C is the O_2-binding to the ^{6}LFeCu catalyst complex.

As well, our kinetics investigations demonstrate that for the Cu-free catalyst, the reduced heme (^{6}LFe) is the species found to be in steady-state. Thus, O_2-binding is rate-determining. However, the rate constant determined (as measured by Fc^{*+} formation) is approximately two times less than that observed with ^{6}LFeCu (Fig. 3*B*). Consequently, the efficiency of the catalyst, as represented by the turnover frequency, is greater for ^{6}LFeCu (TOF = 41 s^{-1}) than that for ^{6}LFe (TOF = 24 s^{-1}). This result suggests that the role of the Cu, at ambient temperature, in this biomimetic catalytic system, is to assist the heme and lead to faster O_2-binding during the catalytic cycle.

We can compare the results here with this heme-Cu C*c*O model compound to systems studied under similar conditions, in homogeneous solutions with ferrocene derivative reductant sources. ^{6}LFeCu offers a significantly higher efficiency (2.2×10^6 s^{-1}, 298 K; slope in Fig. 4*C*) than that observed for previously described cofacial dicobalt porphyrins (320 s^{-1}) or with a mononuclear copper complex (17 s^{-1}) (21–23).

Another role for Cu, as an electron storage and delivery site, was previously proposed by Collman and coworkers based on electrochemical studies (24). This difference may result from the fact that, in the electrochemical approach, the electron flow to the catalyst is controlled, in contrast with our solution homogeneous system. Also, an electrode material supported catalyst may possess a structure modified from that observed in solution (25).

Variable Temperature (VT) Studies. As deduced from Fig. 4*A*, VT studies provide a clearer picture of the change in the rate-determining step for the catalytic $4e^-/4H^+$ reduction of O_2 by Fc* with TFA. At $T < -5$ °C, the O-O bond cleavage of Fe^{III}-OOH is rate-determining.

Because the Cu is not involved here, the zero-order rates (k_{obs}) for ^{6}LFeCu are nearly the same as those of ^{6}LFe (Fig. 4 *A* and *C*). Between −60 and −5 °C (Fig. 4*C*), the activation energy determined for [^{6}LFe^{II}Cu^{I}]$^+$ (9.4 ± 0.1 kcal mol^{-1}) and ^{6}LFe (9.9 ± 0.2 kcal mol^{-1}) are essentially the same.

At higher temperature ($T > -5$ °C), however, the O_2-binding to the reduced species (^{6}LFeCu or ^{6}LFe) becomes rate-determining. The difference in the k_{obs} value between ^{6}LFeCu and ^{6}LFe becomes larger with an increase in temperature and at physiological temperature (37 °C) the k_{obs} value for ^{6}LFeCu becomes seven times larger than that of ^{6}LFe.

Fig. 4*B* shows the change in Soret band as a function of reaction temperature. This phenomenon clearly represents a change in the identity of the steady-state complex for the low and higher temperature processes: The 415–417 nm absorption representing the Fe^{III}-OOH complex in steady-state, shifts to 422–424 nm, identified as the reduced (Fe^{II}) heme complex. Notably, and showing the consistency of our findings and conclusions, the boundary temperature is about −5 °C for the different analyses represented by Fig. 4 *A*–*C*.

Kinetic analyses and Arrhenius plots (Fig. 4*C*) show that the catalytic O_2-reduction using ^{6}LFeCu gives an activation energy of 4.2 ± 0.1 kcal mol^{-1}, between −5 and 35 °C. However, with the ^{6}LFe catalyst, k_{obs} values for O_2-binding decrease with increasing temperature affording an apparent negative activation energy of −3.0 ± 0.1 kcal mol^{-1}. Although the rate of Fc^{*+} formation obeys approximately zero-order kinetics, a more careful examination of the data for ^{6}LFe reveals that the apparent zero-order rate constant increases with increasing Fc* concentration (Fig. 3*C*, Fig. S11*B*). By contrast, for ^{6}LFeCu, the zero-order rate constant remains the same under such conditions (Fig. 4*C*, Fig. S11*A*). These observations indicate that the binding of

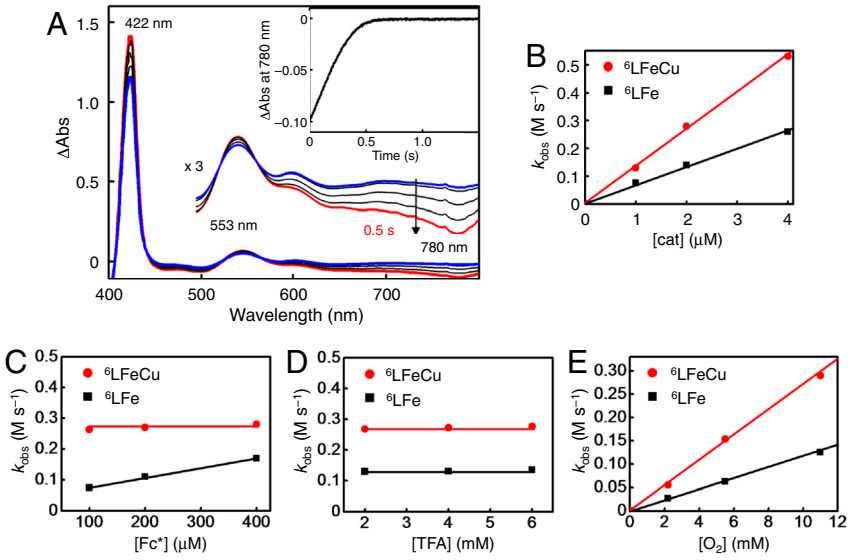

Fig. 3. (*A*) Stopped-flow measurement of the absorbance changes during catalytic O_2-reduction by Fc* (200 μM) with ^{6}LFeCu (2.0 μM), TFA (4 mM) in O_2-saturated acetone at 25 °C. The insert shows the time profile of the absorbance at 780 nm relative to Fc^{*+} formation. See the Fig. 2*A* legend for the explanation of the nonzero ferrocenium concentration initially observed. (*B*) Plots of k_{obs} vs. [cat] for ^{6}LFeCu and ^{6}LFe at 25 °C. (*C*) Plots of k_{obs} vs. [Fc*] for ^{6}LFeCu and ^{6}LFe at 25 °C. (*D*) Plots of k_{obs} vs. [TFA] for ^{6}LFeCu and ^{6}LFe at 25 °C. (*E*) Plots of k_{obs} vs. [O_2] for ^{6}LFeCu and ^{6}LFe at 25 °C.

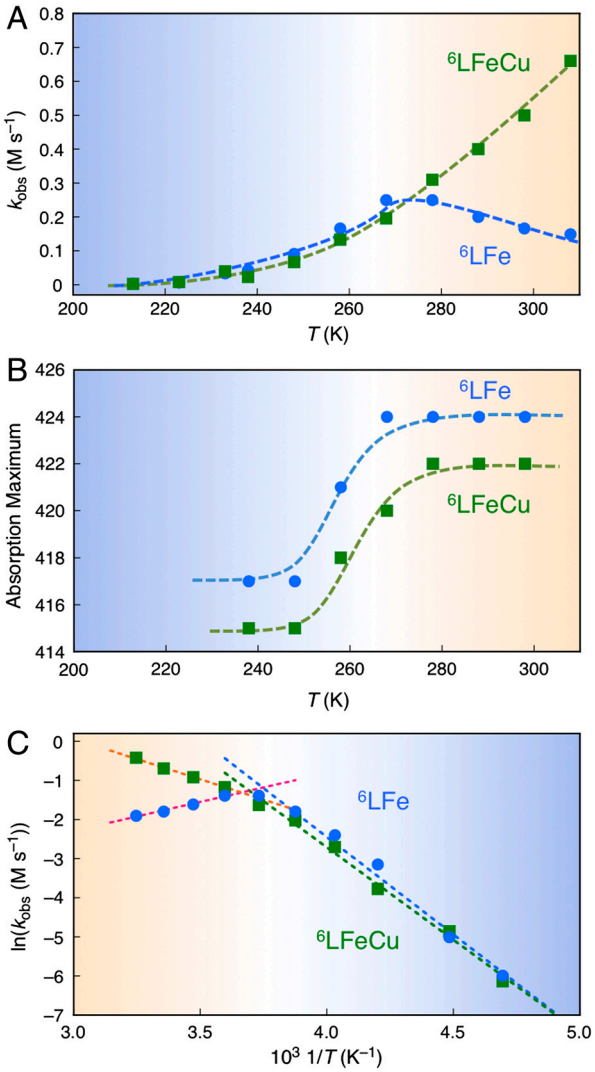

Fig. 4. Plots of k_{obs} vs. temperature for the four-electron reduction of O_2 by Fc* (1.0 mM) catalyzed by ^{6}LFeCu or ^{6}LFe (1.0 μM) in the presence of TFA (1.0 mM) in an air-saturated acetone. (*B*) Plots of the absorbance maximum vs. temperature corresponding to the Soret band of steady-state in the case of ^{6}LFeCu and ^{6}LFe. (*C*) Arrhenius plots obtained by conversion of plots (*A*).

O_2 to ^{6}LFe may be in an equilibrium process and the subsequent electron-transfer reduction of a ^{6}LFe-O_2 intermediate competes with the back reaction (i.e., releasing O_2). Because the O_2-binding is likely an exothermic process, the back reaction (i.e., releasing O_2) becomes faster than the electron transfer as the temperature increases. In such a case, for ^{6}LFe, the overall reaction rate will decrease with an increase in temperature (Fig. 4*A*), thus the negative activation energy.

In light of all the results we suggest a mechanism for the $4e^-/4H^+$ reduction of O_2 catalyzed by our C*c*O active site model (^{6}LFeCu) in the presence of Fc* and TFA in acetone, Fig. 5*A*. All species have been spectroscopically identified, and the interconversions characterized by the detailed kinetic studies. In the presence of acid, [^{6}LFe^{III}-O-Cu^{II}]$^+$ rapidly forms [^{6}LFe^{III}Cu^{II}]$^{3+}$ (409, 505 nm, Fig. S5) releasing water and the catalytic cycle starts via a fast reduction of the heme and then the Cu to generate the reduced complex [^{6}LFe^{II}Cu^{I}]$^+$; as discussed, this corresponds to the steady-state species at RT. The O_2-binding in the next step is rate-determining at RT. The [^{6}LFe^{III}-(O_2^{2-})-Cu^{II}]$^+$ complex thus generated undergoes a fast protonation to form {^{6}LFe^{III}-OOH Cu^{II}}$^{2+}$ corresponding to the low temperature steady-state species. An additional two equiv of Fc* and three

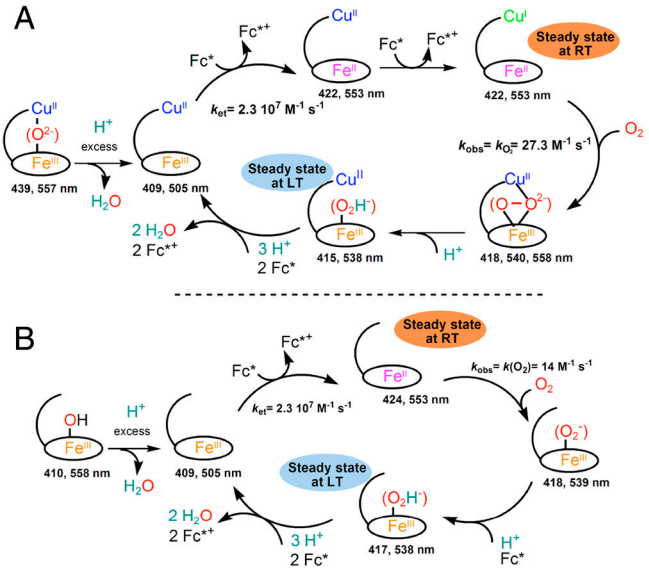

Fig. 5. The proposed mechanism of the four-electron reduction of O_2 to water by Fc* in the presence of TFA in acetone catalyzed by: (*A*) the heme/Cu bimetallic center model of C*c*O (^{6}LFeCu), (*B*) the Cu-free version (^{6}LFe). In fact, it has not yet been established as to which side of the heme the O_2-binding occurs.

protons are needed to complete the $4e^-/4H^+$ reduction of O_2 to water and regenerate the [^{6}LFe^{II}Cu^{I}]$^+$ catalyst.

In the case of ^{6}LFe, the Cu-free catalyst version, the cycle (Fig. 5*B*) also starts via fast electron transfer from Fc* to the heme, forming ^{6}LFe^{II}. In the absence of the Cu, however, as discussed, the subsequent O_2-binding is slower than that observed for [^{6}LFe^{II} Cu^{I}]$^+$. Once an O_2-adduct forms [formally an Fe^{III}-superoxo species (418, 539 nm) (16)], subsequent electron transfer and protonation leads to Fe^{III}-OOH, in steady-state at low temperature. Thus, the important role of Cu is to facilitate the O_2- binding to ^{6}LFe^{II}, directly increasing the rate of this reaction and stabilizing the resulting [^{6}LFe^{III}-(O_2^{2-})-Cu^{II}]$^+$ complex at ambient temperature. As seen for the ^{6}LFeCu catalyst, the rate-determining step changes at low temperature, from O_2-binding to O-O bond cleavage in the Fe^{III}-OOH complex. Cu does not influence this latter step.

In fact, this conclusion about the role of Cu agrees with other notable findings: (*i*) O_2-binding to copper complexes can occur at near diffusion-controlled rates (26, 27), (*ii*) C*c*O enzyme studies in fact implicate Cu_B as the entry point for O_2 during catalysis (28–30).

Conclusion

In summary, we have here described a selective and efficient (turnovers >1,000) four-electron reduction of O_2 to water (without formation of H_2O_2) catalyzed by our C*c*O active site analogue (^{6}LFeCu). Unprecedented direct observation of different reactive intermediates taking part in the catalytic cycle [i.e., ^{6}LFe^{II} (Cu^{I}) and {^{6}LFe^{III}-OOH(Cu)}], depending on the temperature of the system, combined with detailed kinetics studies of different steps of the catalytic reaction when comparing ^{6}LFeCu and its Cu-free version allowed us to obtain unique mechanistic insights. Important conclusions that may relate to C*c*O chemistry are that in our model system the role for the Cu is to enhance the O_2-binding and that it needs not contribute directly to the O-O cleavage process. As no model system can prove a mechanism for an enzyme, our chemistry provides that further systematic variations in the architecture or nature of the synthetic heme-copper catalyst [such as changes in the heme type, Cu-ligand denticity, N-donor type, neighboring groups which can H-bond or alter the local dielectric, or H• ($H^+ + e^-$) donors] can and will

lead to further insights into O_2 reductive activation relevant to C*c*O or fuel cell chemistry.

Materials and Methods

Materials. Grade quality solvents and chemicals were obtained commercially and used without further purification unless otherwise noted. Decamethylferrocene (Fc*) (99%) was purchased from STREM, USA, TFA (99%) from Sigma Aldrich and NaI (99.5%) from Wako, Japan. Acetone was purchased from Wako, Japan and used whether without further purification for non-air-sensitive experiment or dried and distilled under argon then deoxygenated by bubbling with argon for 30–45 min for air-sensitive experiment. Preparation and handling of air-sensitive compounds were performed under MBraun UNilab inert atmosphere (<1 ppm O_2, <1 ppm H_2O) glove box filled with nitrogen. The complexes $[^6LFe^{II}Cu^{I}]^+$ and $^6LFe^{II}$ were prepared according to the literature procedure (14, 15).

UV-Vis Spectroscopy Measurements. Hewlett Packard 8453 diode array spectrophotometer with a quartz cuvette (path length = 10 mm) was used to examine the spectral change in the UV-visible. This instrument was coupled to Unisoku thermostated cell holder for low-temperature experiments. In a typical catalytic reaction, the quartz cuvette is loaded with 3 mL of 1:1 Fc*/TFA (1 mM) in air-saturated solution of acetone. Then 30 μL of 0.1 mM solution of the catalyst in acetone is injected into the cuvette under vigorous stirring. The catalytic reaction is monitored by the increase in the absorbance at 780 nm corresponding to the formation of the ferrocenium cation (Fc^{*+}).

The limiting concentration of O_2 in an acetone solution was prepared by a mixed gas flow of O_2 and N_2. The mixed gas was controlled by using a gas mixer (Kofloc GB-3C, KOJIMA Instrument Inc.), which can mix two or more gases at a certain pressure and flow rate.

Stopped-Flow Measurements. Stopped-flow measurements were performed on a UNISOKU RSP-601 stopped-flow spectrophotometer with an MOS-type high selective photodiode array at various temperatures (248 K–298 K) using a Unisoku thermostated cell holder designed for low-temperature experiments. In a typical reaction, two reactant solutions for stopped-flow mixing were prepared. One is solution containing TFA and the catalyst in acetone, the other is solution Fc* in acetone. Rates of O_2 reduction reactions were determined by monitoring the appearance of the absorption band at 780 nm due to the formation of Fc^{*+}.

ESI-MS Measurements. The detailed information about ESI-MS is provided in *SI Text*.

EPR Measurements. To a reaction solution of $[^6LFe^{III}\text{-}(O_2)\text{-}Cu^{II}]^+$ (Fig. S3) or $[^6LFe^{III}\text{-}(O)\text{-}Cu^{II}]^+$ (1.0 mM) (Fig. S14) in acetone solution, 10 equiv of TFA (10 mM) was added at RT. The resulting solution in the quartz ESR tube (3.0 mm i.d.) was frozen in liquid nitrogen. EPR spectrum recorded at 77 K was taken on a JEOL X-band spectrometer (JES-RE1XE) under nonsaturating microwave power conditions (1.0 mW) operating at 9.2025 GHz (Fig. S14) or a Bruker EMX spectrometer operating at X-band using microwave frequencies around 9.5 GHz (Fig. S3). The magnitude of the modulation was chosen to optimize the resolution and the signal to noise ratio (S/N) of the observed spectrum (modulation width, 20 G; modulation frequency, 100 kHz).

ACKNOWLEDGMENTS. This research was supported by a Grant-In-Aid 20108010 (S.F.), the Global Centers of Excellence (COE) Program from the Ministry of Education, Culture, Sports, Science and Technology, Japan (to Z.H. and S.F.), by the National Institutes of Health (GM28962 to K.D.K.), and World Class University (WCU) Program R31-2008-000-10010-0 (to K.D.K. and S.F.).

1. Ferguson-Miller S, Babcock GT (1996) Heme/copper terminal oxidases. *Chem Rev* 96:2889–2908.
2. Tsukihara T, et al. (1995) Structures of metal sites of oxidized bovine heart cytochrome *c* oxidase at 28 A. *Science* 269:1069–1074.
3. Yoshikawa JS, et al. (1998) Redox-coupled crystal structural changes in bovine heart cytochrome *c* oxidase. *Science* 280:1723–1723.
4. Pereira MM, Santana M, Teixeira M (2001) A novel scenario for the evolution of haem-copper oxygen reductases. *Biochim Biophys Acta* 1505:185–208.
5. Cracknell JA, Vincent KA, Armstrong A (2008) Enzymes as working or inspirational electrocatalysts for fuel cells and electrolysis. *Chem Rev* 108:2439–2461.
6. Willner I, Yan YM, Willner B, Tel-Vered R (2009) Integrated enzyme-based biofuel cells-A review. *Fuel Cells* 9:7–24.
7. Anson FC, Shi A, Steiger B (1997) Novel multinuclear catalysts for the electroreduction of dioxygen directly to water. *Acc Chem Res* 30:437–444.
8. Kim E, Chufán EE, Kamaraj K, Karlin KD (2004) Synthetic models for heme-copper oxidases. *Chem Rev* 104:1077–1134.
9. Chufán EE, Puiu SC, Karlin KD (2007) Heme-copper/dioxygen adduct formation, properties, and reactivity. *Acc Chem Res* 40:563–572.
10. Collman JP, Boulatov R, Sunderland CJ, Fu L (2004) Functional analogues of cytochrome *c* oxidase, myoglobin, and hemoglobin. *Chem Rev* 104:561–588.
11. Collman JP, Boulatov R, Sunderland CJ (2003) *The Porphyrin Handbook*, eds KM Kadish, KM Smith, and R Guilard (Academic Press, San Diego, CA), Vol. 11, pp 1–49.
12. Collman JP, Ghosh S, Dey A, Decreau RA, Yang Y (2009) Catalytic reduction of O_2 by cytochrome *c* using a synthetic model of cytochrome *c* oxidase. *J Am Chem Soc* 131:5034–5035.
13. Chishiro T, et al. (2003) Isolation and crystal structure of a peroxo-bridged heme-copper complex. *Angew Chem Int Ed* 42:2788–2791.
14. Ju TD, et al. (1999) Dioxygen reactivity of fully reduced $[LFe^{II}\cdots Cu^{I}]^+$ complexes utilizing tethered tetraarylporphyrinates: active site models for heme-copper oxidases. *Inorg Chem* 38:2244–2245.
15. Ghiladi RA, et al. (1999) Formation and characterization of a high-spin heme-copper dioxygen (peroxo) complex. *J Am Chem Soc* 121:9885–9886.
16. Ghiladi RA, Karlin KD (2002) Low-temperature UV-visible and NMR spectroscopic investigations of O_2 binding to $(^6L)Fe^{II}$, a ferrous heme bearing covalently tethered axial pyridine ligands. *Inorg Chem* 41:2400–2407.
17. Shigehara K, Anson FC (1982) Electrocatalytic activity of three iron porphyrins in the reduction of dioxygen and hydrogen peroxide at graphite cathodes. *J Phys Chem* 86:2776–2783.
18. Shi CN, Anson FC (1990) Catalytic pathways for the electroreduction of oxygen by iron tetrakis(4-N-methylpyridyl)porphyrin or iron tetraphenylporphyrin adsorbed on edge plane pyrolytic graphite electrodes. *Inorg Chem* 29:4298–4305.
19. Ricard D, Andrioletti B, L'Her M, Boitrel B (1999) Electrocatalytic reduction of dioxygen to water by tren-capped porphyrins, functional models of cytochrome *c* oxidase. *Chem Commun* 1523–1524.
20. Ricard D, L'Her M, Ricard P, Boitrel B (2001) Iron porphyrins as models of cytochrome *c* oxidase. *Chem Eur J* 7:3291–3297.
21. Fukuzumi S, Okamoto K, Gros CP, Guilard R (2004) Mechanism of four-electron reduction of dioxygen to water by ferrocene derivatives in the presence of perchloric acid in benzonitrile, catalyzed by cofacial dicobalt porphyrins. *J Am Chem Soc* 126:10441–10449.
22. Rosenthal J, Nocera DG (2007) Role of proton-coupled electron transfer in O-O bond activation. *Acc Chem Res* 40:543–553.
23. Fukuzumi S, et al. (2010) Mononuclear copper complex-catalyzed four-electron reduction of oxygen. *J Am Chem Soc* 132:6874–6875.
24. Collman JP, et al. (2007) A cytochrome *c* oxidase model catalyzes oxygen to water reduction under rate-limiting electron flux. *Science* 315:1565–1568.
25. Kadish KM, et al. (2009) Catalytic activity of biscobalt porphyrin-corrole dyads toward the reduction of dioxygen. *Inorg Chem* 48:2571–2582.
26. Fry HC, Scaltrito DV, Karlin KD, Meyer GJ (2003) The rate of O_2 and CO binding to a copper complex, determined by a "flash-and-trap" technique, exceeds that for hemes. *J Am Chem Soc* 125:11866–11871.
27. Lucas HR, Meyer GJ, Karlin KD (2010) CO and O_2 binding to pseudo-tetradentate ligand-copper(i) complexes with a variable N-donor moiety: kinetic/thermodynamic investigation reveals ligand-induced changes in reaction mechanism. *J Am Chem Soc* 132:12927–12940.
28. Blackmore RS, Greenwood C, Gibson QH (1991) Studies of the primary oxygen intermediate in the reaction of fully reduced cytochrome oxidase. *J Biol Chem* 266:19245–19257.
29. Oliveberg M, Malmström BG (1992) Reaction of dioxygen with cytochrome *c* oxidase reduced to different degrees: indications of a transient dioxygen complex with copper-B. *Biochemistry* 31:3560–3563.
30. Muramoto K, et al. (2010) Bovine cytochrome *c* oxidase structures enable O_2 reduction with minimization of reactive oxygens and provide a proton-pumping gate. *Proc Nat Acad Sci USA* 107:7740–7745.